

THz MMICs based on InP HBT Technology

Jonathan Hacker, Munkyo Seo, Adam Young, Zach Griffith, Miguel Urteaga,
Thomas Reed, and Mark Rodwell.

Abstract—An indium-phosphide (InP) double-heterojunction bipolar transistor (DHBT) based suite of terahertz monolithic integrated circuits (TMICs) fabricated using 256nm InP DHBT transistors and a multipurpose three metal layer interconnect system is reported. The InP DHBT MMIC process is well suited for TMICs due to its high bandwidth ($f_{max} = 808$ GHz) and high breakdown voltage ($BVC_{Bo} = 4V$) and integrated 10- μm thick layer of BCB dielectric supporting both low-loss THz microstrip lines for LNA, PA, and VCO tuning networks, and high-density thin-film interconnects for compact digital and analog blocks. TMIC low noise and driver amplifiers, fixed and voltage controlled oscillators, dynamic frequency dividers, and double-balanced Gilbert cell mixers have been designed and fabricated. These results demonstrate the capability of 256nm InP DHBT technology to enable sophisticated single-chip heterodyne receivers and exciters for operation at THz frequencies.

Index Terms—Submillimeter-wave, terahertz, TMIC, indium phosphide (InP) double-heterojunction bipolar transistor (DHBT).

I. INTRODUCTION

SUBMILLIMETER-WAVE and terahertz bands covering a frequency range from 0.3 to 3 GHz are associated with a broad range of potential applications including imaging, radar, spectroscopy, and communications [1,2]. To date, the realization of circuit components for this band has been dominated by two-terminal devices such as Schottky diodes mounted in individually machined high precision waveguide blocks and ganged together to form functional blocks to realize a receiver or exciter. Such circuit implementations are bulky, costly to manufacture, and time consuming to assemble with low repeatability and integration densities preventing their use in many applications.

During the 1970's, the development of the microwave monolithic integrated circuit (MMIC) enabled the implementation of complex transistor-based microwave circuits monolithically integrated onto a single chip and thereby revolutionized the way in which microwave circuits

This work was supported by ARL under Contract No. HR0011-09-C-0060, Alfred Hung Program Manager, and by Mark Rosker, Deputy Director, and John Albrecht, Program Manager, at the Defense Advanced Research Projects Agency (DARPA) Microsystems Technology Office.

J. B. Hacker, M. Seo (formerly UCSB), A. Young, Z. Griffith, and M. Urteaga are with the Teledyne Scientific Company, 1049 Camino Dos Rios, Thousand Oaks, CA 91360, U.S.A. (e-mail: jbhacker@ieee.org).

T. Reed, and M. Rodwell are with the University of California, Santa Barbara, CA 93106-9560, USA.

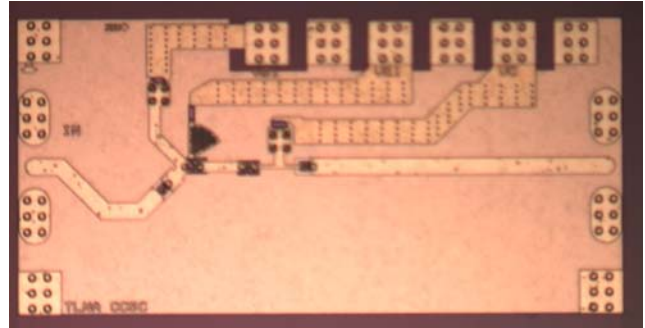


Fig. 1. A photomicrograph of a cascode InP DHBT TMIC for low-noise amplification from 280 to 310 GHz with microstrip lines on thick 10 μm BCB. The compact die measures 1500 μm by 750 μm with a wafer thickness of 50 μm .

are realized. The development of sophisticated MMICs has spawned a broad range of applications in microwave communications and sensors. Therefore, it is reasonable to expect that the development of terahertz monolithic integrated circuits (TMICs) will, likewise, revolutionize circuits and systems in the frequency band from 0.3 to 3 THz and enable the widespread adoption of new and emerging systems applications including active imagers and sensor arrays where compact monolithically integrated circuits are key to realizing the required element spacings and dense functionality.

Historically, the bandwidth (f_{max}) of transistor devices has been below the sub-MMW band, precluding the use of transistor electronics for applications above 300 GHz. However, the bandwidth of InP-based transistors is increasing rapidly. InP HEMTs have attained bandwidths > 1 THz at 35

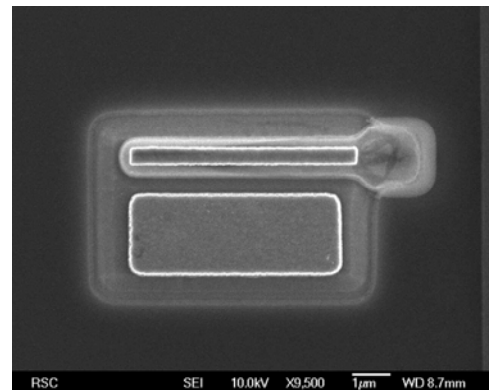


Fig. 2. SEM of 0.256 μm HBT device footprint. The emitter and base contact widths are 400 and 150 nm, respectively. The emitter-base junction width is 300 nm.

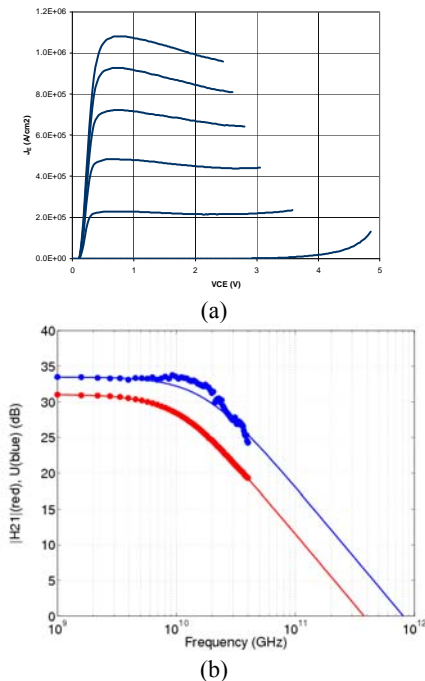


Fig. 3. (a) Measured common-emitter characteristics of a 256nm InP DHBT demonstrating $>4V$ breakdown voltage. (b) Measured unilateral power gain and h_{21} for $0.25 \times 5 \mu\text{m}^2$ HBT used to extrapolate an f_{max} of 808 GHz and an f_t of 378 GHz, respectively.

nm gate length [3]. InP HBTs have attained bandwidths of 808 GHz (Fig. 4) at a much larger 250 nm emitter width while demonstrating $>4V$ breakdown voltage (Fig. 3a). Both technologies will operate at 1.0 THz. However, HBTs have key advantages that enable complex TMICs. Given their high breakdown voltage, high digital speed, and low noise, InP HBTs provide a single IC platform in which all receiver and transmit components (LNA, VCO, mixer, LO PLL) can be constructed. Single-chip construction eliminates THz waveguide connections between circuit blocks. This greatly reduces package size and interconnect losses, and is critical for constructing THz receiver arrays with the needed single-wavelength element spacings for arrays. Furthermore, developing low-noise active electronics at these frequencies would lead to significant improvements in receiver sensitivity compared to today's diode mixer front ends without amplification.

In this paper, we present circuits using deep sub-micron scaled InP HBTs for the eventual realization of fully monolithic exciter and receiver circuits in the terahertz band. HBTs are easily integrated, with excellent threshold uniformities necessary for high-yield monolithic ICs. Because of their wide bandgap InP collector, HBTs attain much higher breakdown voltage than HEMTs at a given f_t . This makes HBTs well suited for power amplifiers and for digital circuits. While the HBT's phase-noise properties are known to be superior to HEMTs, at low frequencies HEMTs show superior

noise figure because of low input shot noise. However, for carrier frequencies approaching a significant fraction of the transistor bandwidth, the HBT noise figure is comparable to a HEMT as well. Low HBT noise is obtained by biasing at ~ 10 -20% of the peak-current densities; this reduces gain only 1-2 dB. These advantages, coupled with a clear path to developing devices for >1 THz operation [4], make InP HBTs a very attractive transistor technology for future THz electronics; especially where a single-chip form-factor and cost are key drivers.

II. DEVICE DESIGN AND CHARACTERIZATION

The DHBT structure is grown using molecular beam epitaxy on four-inch semi-insulating InP substrates (Fig. 2). The epitaxy utilizes a 30nm carbon-doped base layer and a 150nm N-InP collector region [5]. The emitter contact is patterned using electron-beam lithography and formed using an Au-based electroplating process [6]. Dielectric sidewall spacers are formed that passivate the base-emitter junction and permit the formation of a self-aligned base contact. After base-contact deposition, the remaining HBT process flow follows that of a standard mesa-HBT process. The transistors are passivated with a spin-on-dielectric (Benzocyclobutene, BCB) [7]. The HBT IC process includes thin-film resistors ($50 \Omega/\text{sq}$), MIM capacitors, and 3-levels of interconnect. A $10\text{-}\mu\text{m}$ thick BCB layer is used between the 2nd and 3rd interconnect layers to facilitate the formation of low-loss thin-film microstrip lines.

In this work, TMIC results are reported using 3rd generation devices with emitter junction widths of 256nm. Device development of 4th generation 128nm emitter junction widths is underway and preliminary results support the goal of circuit operation at frequencies beyond 400 GHz. The 256nm InP DHBT has a measured dc beta of ~ 30 . In this technology, $0.25 \times 4 \mu\text{m}^2$, on-wafer s-parameter measurements show a cutoff frequency, f_t , of 378 GHz and a maximum oscillation frequency, f_{max} , of 808 GHz (Fig. 3b). Further details on the DHBT structure and performance used in these MMICs have been reported elsewhere [4-6].

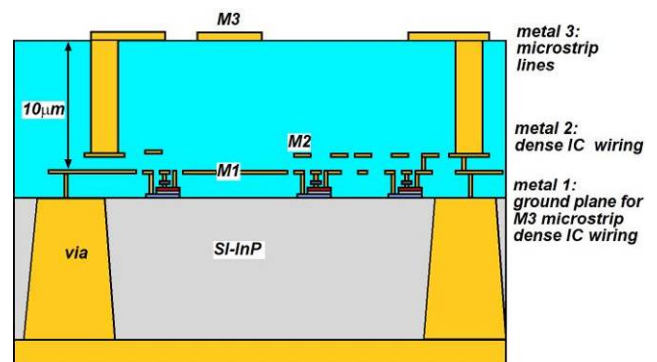


Fig. 4: IC interconnect cross-section showing low-loss THz microstrip lines for LNA, PA, VCO tuning networks and high-density thin-film interconnects for high-density digital blocks.

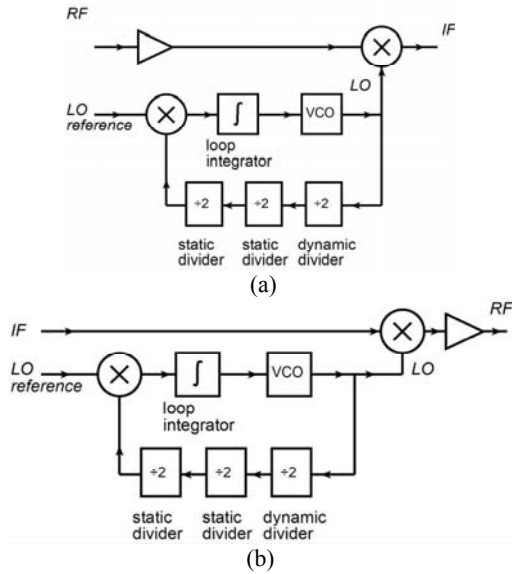


Fig. 5. (a) Receiver front-end block diagram . (b) Transmitter exciter block diagram.

III. THICK BCB TRANSMISSION LINE CIRCUITS

The ICs demonstrated in this paper are only moderately complex; hence need use only three interconnect metal levels (Fig. 4). Our IC demonstrations include both traditional distributed microwave type (PA, LNA), as well as analog-type (single frequency oscillator, VCO, frequency divider) circuits, both operating above 300 GHz, and the wiring requirements for each of these circuit blocks are unique. Lumped-element analog blocks require low-delay, low parasitic wiring and interconnects for these circuits must support narrow lines and fine pitch. The lower two levels (M1, M2), are used mostly for wiring these blocks, and are separated by a 1 μm BCB

interlayer dielectric.

Distributed sub-mm-wave circuits require high Q and low loss transmission lines in the 0.3 to 3 THz band with a wide range of realizable characteristic impedances for the amplifier matching networks. To achieve this, the upper metal level (M3) is separated from those below by a thicker 10 μm BCB layer. The thick BCB layer provides low-loss submillimeter-wave transmission lines with smaller dimensions compared to conventional microstrip placed directly on the thinned semiconductor substrate with a backside ground plane. Additionally, the use of BCB as the microstrip substrate isolates the rf signals of the circuit from the InP carrier substrate, permitting the use of a thicker and, hence, more robust MMIC substrate. Backside processing of through-wafer VIAs is also provided for substrate mode control, especially needed when the TMICs are placed in waveguide based packages.

The low dielectric constant BCB allows for more compact impedance matching and power-combining networks, reducing IC area [8,9] and facilitating low-parasitic

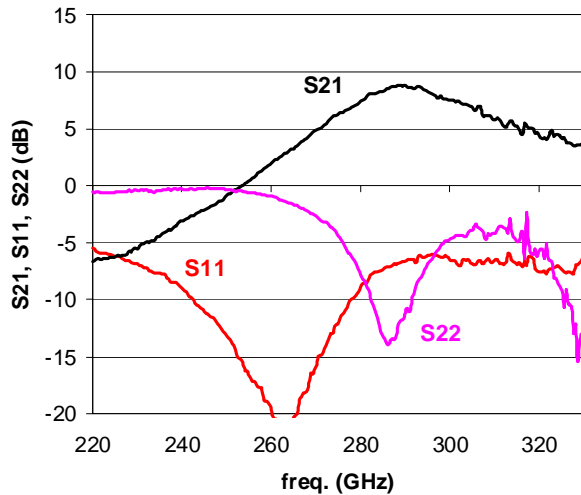


Fig. 6. Measured insertion gain (s21) and input (s11) and output (s22) return loss of the single stage cascode inverted microstrip design compared with the theoretical prediction from circuit model. The well matched LNA gain is 9 dB at 290 GHz.

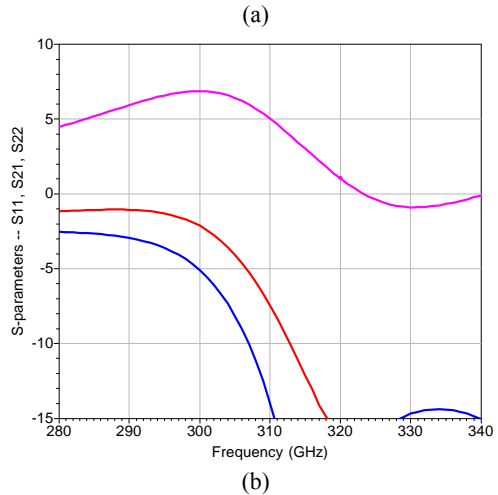
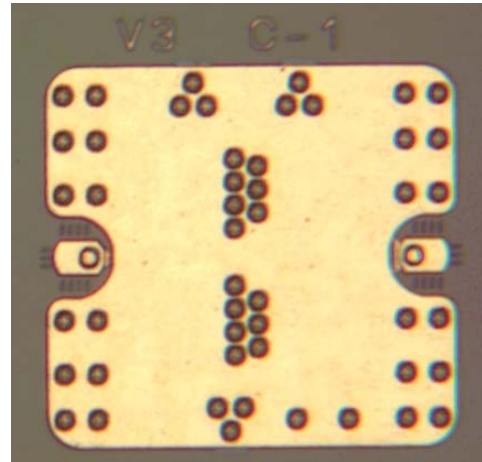


Fig. 7. (a) Photograph of a single stage common base driver amplifier using two finger 0.25 x 5 μm device to produce 7dBm of output power at 300 GHz. (b) Simulated s-parameters for the driver amplifier TMIC.

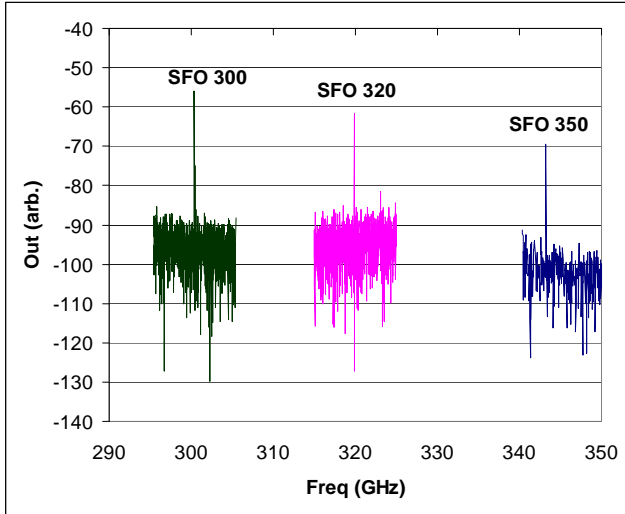


Fig. 8. Plots of measured fixed frequency oscillator signal output for three different designs. Output powers of 312, 205, and 120 μW were measured respectively.

connections to the small active devices. Because the primary skin losses $\alpha_{skin} \propto \epsilon_r^{1/2} / T$ increase as the substrates is thinned for a given Z_0 , reduced die area indirectly results in increased line losses. However, selecting a low ϵ_r substrate such as BCB ($\epsilon_r=2.5$) can reduce the attenuation compared to a typical semiconductor substrate that has an ϵ_r of $\sim 11-13$.

To characterize the thick BCB microstrip rf wiring process, a set of 50Ω microstrip test structures of varying length were fabricated. Measured performance of the lines up to 328 GHz (the limit of our vector network analyzer test set) have been previously published [9]. The measured data shows low loss and good agreement with model predictions for Z_0 . The measured loss (pads deembedded) is 0.88 dB/mm. From this data, the BCB dielectric constant and loss tangent were found to be 2.54 and 0.005 respectively at 300 GHz.

IV. CIRCUIT DESIGN FABRICATION AND TEST

A block diagram of a typical microwave receiver is shown in Fig. 5a consisting of an LNA, mixer, and IF amplifier, while Fig. 5b shows a transmitter exciter containing a mixer and an output amplifier; in both, a PLL generates the LO. In order to realize these systems in the terahertz band, all required circuit blocks need to be demonstrated at frequencies greater than 300 GHz. By using this receiver architecture, as commonly used at RF and microwave frequencies, dramatic improvements in system performance, especially in signal-to-noise ratio (70dB or more), are expected relative to current THz “direct” (rectifying) detector approaches. To validate that our THz HBT technology provides a single IC platform for all the required circuit components, we designed and fabricated LNA and driver amplifiers, mixer, VCO, and divider circuits for operation at 300 GHz.

V. LOW NOISE AND DRIVER AMPLIFIERS

Both single and 2 stage cascode low noise amplifiers were designed for operation at 300 GHz. The cascode designs use $0.25 \times 4\text{-}\mu\text{m}^2$ DHBT devices biased such that the base of the common base device is connected directly to ground for the highest stable gain. The linear small-signal model used for the design was based upon a physics-based VBIC model combined with a proprietary passive external parasitic network fit to measured data. The noise model parameters are obtained directly from the VBIC model, an approach that has previously given good agreement at mm-wave frequencies [10].

The HBT devices used in the amplifier are interconnected with microstrip matching networks. Designs using both normal and inverted microstrip were included. A full-wave 2.5D electromagnetic solver was used to model layout induced effects. Several iterations of design and EM simulation were needed to obtain good simulated amplifier performance. A microphotograph of the single cascode stage device using inverted microstrip is shown in Fig. 1. Measured performance is shown in Fig 6. A peak gain of 9dB was measured from 280

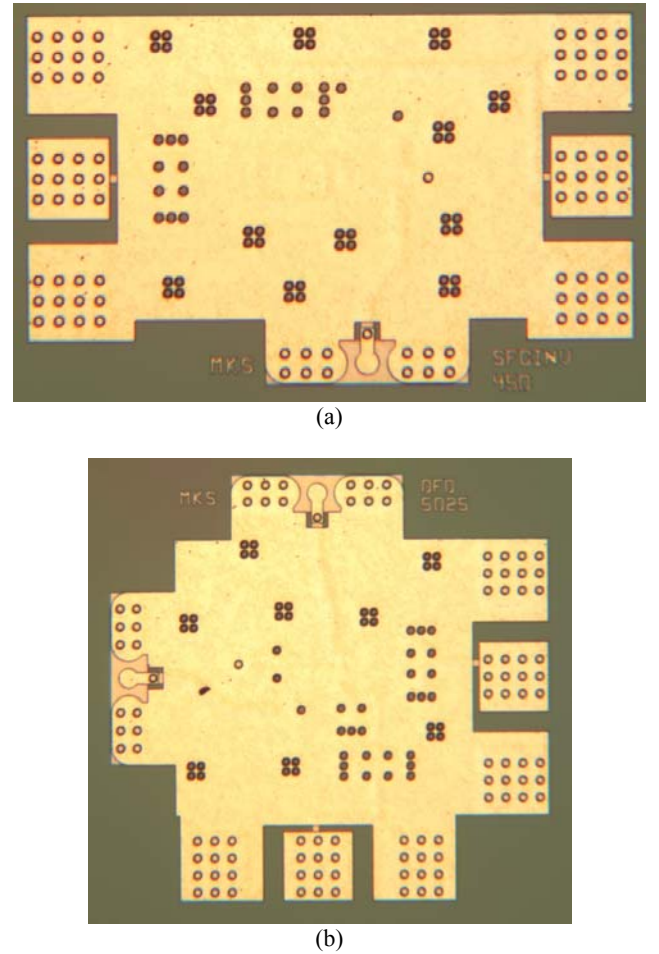


Fig. 9. Photomicrographs of (a) a 350 GHz inverted microstrip single frequency oscillator (SFO) TMIC and (b) a 300 GHz frequency divider TMIC with external rf input.

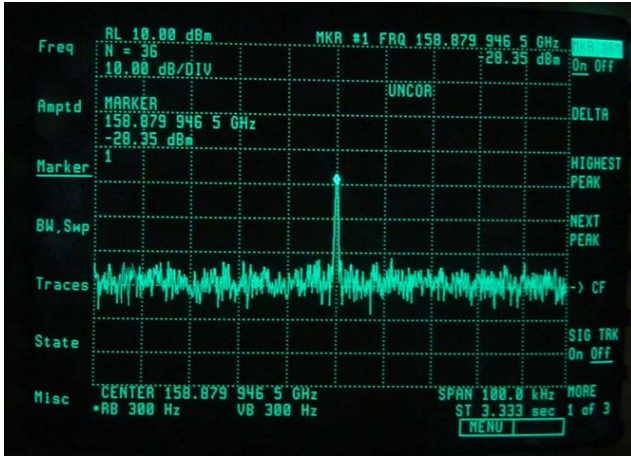


Fig. 10. Measured output spectrum from the divide by 2 dynamic frequency divider when driven with an input frequency of 317.76 GHz at an estimated power level of -3 dBm. The measured divider bandwidth was 312 to 318 GHz.

to 300 GHz. Noise figure measurements are in characterization at the time of publication, but simulated values of 11.3dB are expected.

Driver amplifiers for operation at a frequency of 300GHz and using a 2-finger common-base design, each with emitter dimensions of $0.25 \times 5\mu\text{m}$, with reduced extrinsic parasitics by layout were also designed and fabricated. Fig. 7a shows the compact inverted microstrip single-stage TMIC, while Fig. 7b shows the simulated frequency response. The simulated gain is 7dB at 300 GHz while the 1 dB compression point is 7 dBm. Measurements of gain and output power are in characterization at the time of publication

VI. OSCILLATOR TMIC

Local oscillators (LO) with low phase noise are a critical design challenge in THz receivers. The HBT device, because of its lower $1/f$ noise compared with HEMTs, has the potential for lowest noise. Both single frequency (SFO) and voltage controlled (VCO) oscillators were designed and fabricated for operation from 300 to 500 GHz. The chosen oscillator topology consists of a series-tuned oscillator (T-network feedback) because it is less affected by layout parasitics than a traditional Colpitts configuration, a critical advantage at terahertz frequencies where layout parasitics dominate.

Fig 9(a) shows a microphotograph of the single frequency oscillator TMIC. Fig 8 shows the measured performance of three such TMIC oscillators designed for 300, 320 and 350 GHz. Oscillation frequencies were within 5% of design values, and measured output power of 312, 205, and 120 μW were measured respectively.

Voltage controlled oscillators with 10% tuning range covering bands from 300 to 500 GHz were also designed and fabricated, but measured data was not available at the time of publication.

VII. DYNAMIC FREQUENCY DIVIDER TMIC

Dynamic frequency dividers (DFD) TMICs were designed with a double-balanced mixer with emitter-follower feedback and resonant load topology. The designs are adapted from Hans M. Rein's original circuit. The divide by 2 dividers are designed to operate over a bandwidth from 270 to 370GHz with an rf input power of 0 dBm. The TMICs consume 105mW of dc power at a bias voltage of -4.4V . Dividers were fabricated with both integrated oscillators and standalone with external rf probable inputs (Fig 9b).

Fig 10 shows the measured output spectrum from the DFD TMIC with an input of 317.76 GHz from a VDI multiplier source at an estimate rf power level of -3 dBm. The measured output signal was 158.88 GHz at -28.4 dBm. The limited bandwidth of our VDI rf source prevented us from characterizing the full bandwidth of the DFD TMIC.

VIII. MIXER TMIC

Double balanced Gilbert cell mixers were designed and fabricated to cover the band from 300 to 320 GHz using a 323 GHz local oscillator. Both active and passive balun designs were investigated, but the passive balun was not used because it requires significant space, and is narrowband with losses that impacts the mixer noise figure. The active balun is more compact, but requires a good rf short and requires robust devices to handle the LO power. Fig. 11a shows a photograph of an active balun mixer TMIC. Fig 11b shows the simulated conversion loss and noise figure of the mixer with an rf input frequency of 300 GHz and an LO frequency of 323 GHz. Simulated optimum LO power is -4 to 4 dBm, with a

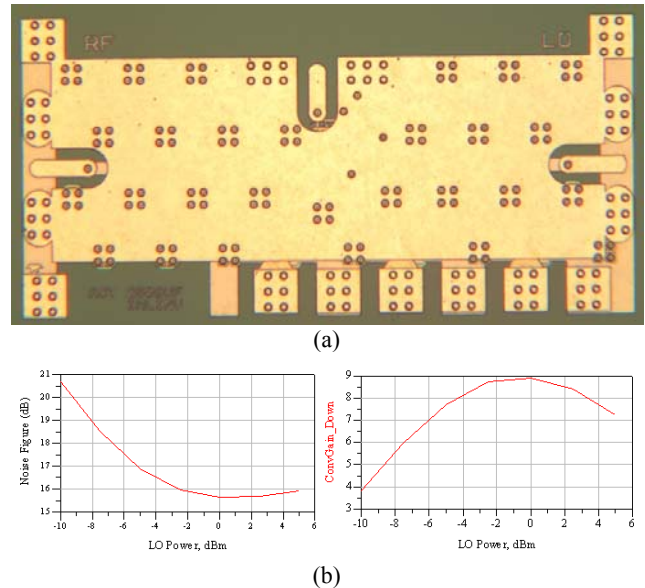


Fig. 11. (a) CAD layout of the double balanced Gilbert cell mixer for operation at 300 to 320 GHz. (b) Simulated noise figure and conversion loss at 300 GHz as a function of LO power for the mixer TMIC.

minimum noise figure of 15.6 dB at 0 dBm, and a corresponding conversion gain of 8.9 dB. The mixer circuits have been fabricated, but measured data was not available at the time of publication.

IX. CONCLUSION

We report on the development of a suite of terahertz monolithic integrated circuits (TMICs) fabricated using 256nm InP DHBT transistors and a multipurpose three metal layer interconnect system. The InP DHBT MMIC process is well suited for TMICs due to its high bandwidth ($f_{max} = 808$ GHz) and high breakdown voltage ($BVC_{Bo} = 4V$) and integrated 10- μ m thick layer of BCB dielectric supporting both low-loss THz microstrip lines for LNA, PA, VCO tuning networks and high-density thin-film interconnects for high-density digital and analog blocks. TMIC low noise amplifiers, driver amplifiers, fixed and voltage controlled oscillators, dynamic frequency dividers, and double-balanced Gilbert cell mixer have been designed and fabricated. These results demonstrate the capability of 256nm InP DHBT technology to enable single-chip heterodyne receivers and exciters for operation above 300 GHz.

ACKNOWLEDGMENT

The authors thank R. Pierson for device development, D. Deakin and the Teledyne Scientific Electronics cleanroom staff for device fabrication, and P. Rowell and P. Chen for device measurement. The views, opinions and/or findings contained in this article are those of the authors and should not be interpreted as representing the official views or policies, either expressed or implied, of the Defense Advanced Research Projects Agency or the Department of Defense.

REFERENCES

[1] <http://www.darpa.mil/mto/programs/thz/index.html>
 [2] L. Samoska, "Towards Terahertz MMIC Amplifiers: Present Status and Trends," *2006 IEEE MTT-S International Microwave Symposium Digest*, pp.333-336, June 2006
 [3] R. Lai, W.R. Deal, X.B. Mei, W. Yoshida, J. Lee, L. Dang, J. Wang, Y. M. Kim, P.H. Liu, V. Radisic, M. Lange, T. Gaier, L. Samoska, A. Fung, "Fabrication of InP HEMT Devices with Extremely High f_{max} ," *IEEE/LEOS Int. Conf. Indium Phosphide and Related Materials*, Versailles, France, May 2008
 [4] Rodwell, M.J.W, Minh Le, Brar B., "InP Bipolar ICs: Scaling Roadmaps, Frequency Limits, Manufacturable Technologies," *Proceedings of the IEEE*, vol.96, no.2, Feb. 2008, pp.271-286
 [5] Zach Griffith, Erik Lind, and Mark J.W. Rodwell: "Sub-300nm InGaAs/InP Type-I DHBTs with a 150 nm collector, 30 nm base demonstrating 755 GHz f_{max} and 416 GHz f_t " *IEEE/LEOS Int. Conf. Indium Phosphide and Related Materials*, Matsue, Japan, May 14-18, 2007
 [6] M. Urteaga, P. Rowell, R. Pierson, B. Brar, M. Dahlstrom, Z. Griffith, M.J. Rodwell, S. Lee, N. Nguyen, C. Nguyen, "Deep Submicron InP DHBT Technology with Electroplated Emitter and Base Contacts," *62nd DRC. Conf. Dig. Device Research Conference*, pp. 21-23, June 2004

[7] The Dow Chemical Company, Dow Center, Midland, MI 48674, 1-800-232-2436
 [8] V.B. Krishnamurthy, H.S. Cole, T. Sitnik-Nieters, "Use of BCB in High Frequency MCM Interconnects," *IEEE Trans. Comp., Pack., Manuf. Tech., Part B. Adv. Pack.*, vol. 19, no. 1, pp. 42-47, Feb 1996
 [9] J. Hacker, W. Ha, C. Hillman, M. Urteaga, R. Pierson, B. Brar, "Compact InP HBT Power Amplifiers Using Integrated Thick BCB Dielectrics," *2007 IEEE MTT-S International Microwave Symposium Digest*, pp.805-808, June 2007
 [10] S.P. Voinigescu, M.C. Maliepaard, J.L. Showell, G.E. Babcock, D. Marchesan, M. Schroter, P. Schvan, D.L. Hareme, "A Scalable High-Frequency Noise Model for Bipolar Transistors with Application to Optimal Transistor Sizing for Low-noise Amplifier Design" *IEEE Journal of Solid-State Circuits*, Volume 32, Issue 9, Sept. 1997 Page(s):1430 - 1439